Cationic side-chains control DNA/RNA binding properties and antiproliferative activity of dicationic dibenzotetraaza[14]annulene derivatives†

Marijana Radić Stojković,[a] Marko Marjanović,[c] Dariusz Pawlica,[b] Lukasz Dudek,[b] Julita Eilmes,[b] Marijeta Kralj[c] and Ivo Piantanida*[a]

Received (in Montpellier, France) 17th September 2009, Accepted 23rd November 2009
First published as an Advance Article on the web 15th January 2010
DOI: 10.1039/b9nj00490d

Studied dicationic dibenzotetraaza[14]annulene derivatives intercalate into synthetic double stranded DNA and RNA, while their positively charged side-chains additionally interact within the minor groove of polynucleotides, contributing to the overall affinity of compounds and controlling pronounced A–T(U) over G–C sequence preference as well as stronger thermal stabilization of ds-DNA than ds-RNA. Furthermore, all compounds showed moderate to high antiproliferative activity against five human tumour cell lines, whereby clear correlation between the structure of the side-chain and cytotoxic activity was observed.

1. Introduction

Nucleic acids, particularly DNA, but also on a growing scale RNA, are prime targets for several major categories of drugs in the areas of infections and cancer.[1] Although general patterns of recognition are now appreciated, subtle structural features important to the DNA binding affinity or selectivity and the ensuing effects are still being unravelled.[2] In spite of the advances, the *de novo* design of sequence-selective DNA binding agents is not yet straightforward, and the derivation of therapeutic compounds (*e.g.*, antitumor drugs) remains an even more complex task. Therefore, the search for a new lead small molecule either from natural sources or based on up-till-now untapped small organic molecules is of the utmost interest, whereby application of numerous methods and approaches is necessary for accurate determination of binding modes and affinity.[3]

Cationic porphyrins are promising and intensively studied class of DNA-binding molecules with potential applications in biology and medicine, in particular, as potent *anti*-viral and antitumor therapeutic agents.[4] As DNA binding ligands, porphyrins are quite unusual; they may associate with DNA in three distinct binding modes, which include intercalation, groove binding, and outside binding with self-stacking along the DNA helix.[5] However, surprisingly little is known about DNA binding properties and biological activity of close analogues of porphyrins-dibenzotetraaza[14]annulenes (DBTAA), although the structure, rather simple synthesis and modification procedures, along with metal cation binding ability clearly reveal the biological potential of DBTAA derivatives. Therefore, recently we have reported on synthesis, crystal structures, DNA/RNA binding and antiproliferative activity of a series of bis-cationic DBTAA derivatives (**1–3**).[6,7] The antiproliferative effect of **1–3** on human tumor and normal cell lines was in a good agreement with the strength of observed interactions of **1–3** with DNA/RNA, whereby **2** revealed the most interesting properties. Based on the structure of **2**, a new series of compounds was prepared (**4–7**) (Scheme 1), with the idea that fine tuning of the length, rigidity and positive charge exposure of cationic substituents attached to DBTAA core could lead to novel DNA/RNA binding properties and eventually to increased antiproliferative activity. Very recent preliminary results revealed improved DNA binding properties of **4–7**[8] in comparison with first generation of cationic DBTAA derivatives **1–3**.[7] Here we present a detailed study of **4–7** interactions with synthetic DNA and RNA as well as the screening of their antiproliferative activity.

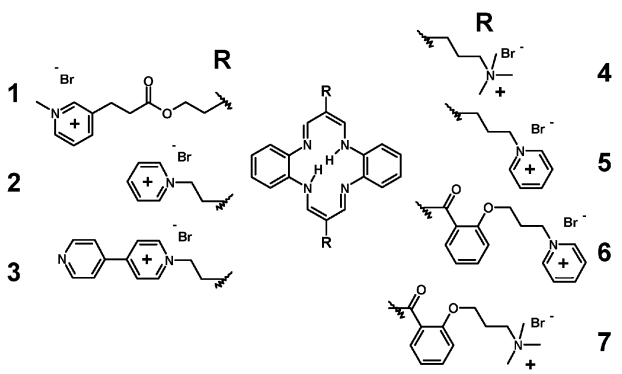

Scheme 1 Cationic, DNA/RNA active DBTAA derivatives: the first (**1–3**)[7] and second (**4–7**)[8] generation.

[a] *Division of Organic Chemistry and Biochemistry, Ruđer Bošković Institute, Bijenička cesta 54, PO Box 180, HR-10002 Zagreb, Croatia. E-mail: pianta@irb.hr*
[b] *Department of Chemistry, Jagiellonian University, Ingardena 3, 30-060 Kraków, Poland. E-mail: jeilmes@chemia.uj.edu.pl*
[c] *Division of Molecular Medicine, Ruđer Bošković Institute, Bijenička cesta 54, P. O. Box 180, HR-10002 Zagreb, Croatia. E-mail: mhorvat@irb.hr*

† Electronic supplementary information (ESI) available: Solubility measurements, spectrophotometric titration curves and viscometry measurements. See DOI: 10.1039/b9nj00490d

2. Results and discussion

2.1 Spectrophotometric titrations of 4–7 with ds-DNA and ds-RNA in aqueous medium

Compounds **4**, **5**, **6** and **7** were previously characterized in aqueous medium by several spectrophotometric methods and were shown to be stable in biologically relevant conditions.[8] Moreover, preliminary experiments showed that **4**, **5**, **6** and **7** interact strongly with ds-DNA.[8] Studies presented here with synthetic ds-DNA and ds-RNA sequences revealed that addition of any ds-polynucleotide resulted in strong batho-chromic and hypochromic effects of UV/Vis spectra of studied compounds (Fig. 1, spectral changes are summarized in Table 1), which are in general not significantly dependent on the basepair composition of the polynucleotide and do not distinguish between DNA and RNA. It is noteworthy that isosbestic points are observed in the most UV/Vis titrations in the region where only the studied compounds absorb light ($\lambda > 300$ nm), pointing to the formation of one dominant type of complex.

The binding constants K_s and ratios $n_{[\text{bound compound}]/[\text{DNA/RNA}]}$ obtained by processing of UV/Vis titration data with the Scatchard equation[9] are summarized in Table 2. In general, **4–7** showed similar affinity toward ds-DNA and ds-RNA. The

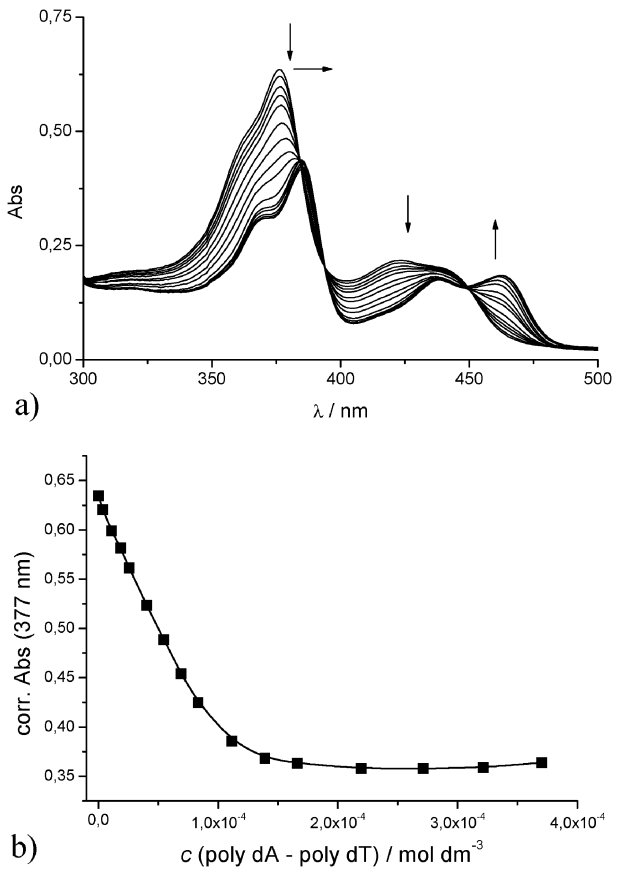

Fig. 1 (a) Changes in UV/Vis spectrum of **4** ($c = 1.53 \times 10^{-5}$ mol dm^{-3}) upon titration with poly dA–poly dT; (b) Agreement between UV/Vis titration data ($\lambda_{max} = 377$ nm) of **4** with poly dA–poly dT (■) and calculated data by non-linear fitting to Scatchard equation (—), pH = 7, sodium cacodylate buffer, $I = 0.05$ mol dm^{-3}.

Table 1 Spectroscopic changes of the UV/Vis spectra of **4–7** observed in titrations with ds-polynucleotides (pH = 7.0, buffer sodium cacodylate, $I = 0.05$ mol dm^{-3})

	poly dA–poly dT			poly A–poly U			poly G–poly C		
		$\Delta\lambda^a$/nm			$\Delta\lambda^a$/nm			$\Delta\lambda^a$/nm	
Compound	H^b (%)	$\Delta\lambda_1$	$\Delta\lambda_2$	H^b (%)	$\Delta\lambda_1$	$\Delta\lambda_2$	H^b (%)	$\Delta\lambda_1$	$\Delta\lambda_2$
4	44	8	15	42	10	14	31	2	10
5	27	6	5	37	4	6	40	5	4
6	26	4	—	21	11	—	39	−10	—
7	29	6	—	23	13	—	43	−10	—

[a] $\Delta\lambda = \lambda$(**4**, **5**, **6** and **7**) − λ(complex); absorbance maxima λ_1 ($4_{\lambda 377\,nm}$, $5_{\lambda 385\,nm}$, $6_{\lambda 346\,nm}$, $7_{\lambda 344\,nm}$) λ_2 = ($4_{\lambda 424\,nm}$, $5_{\lambda 438\,nm}$). [b] Hypochromic effect calculated by Scatchard for **4**, **5**, **6** and **7**; H = (Abs(**4**, **5**, **6** and **7**) − Abs(complex))/Abs(**4**, **5**, **6** and **7**)) × 100.

compounds **4** and **5** bind to poly A–poly U somewhat stronger than to poly G–poly C, and in line with that is the somewhat higher affinity of these compounds toward poly dA–poly dT than toward ct-DNA which contains a significant percentage of dG–dC basepairs. The compounds **6** and **7** also show pronounced poly A–poly U over poly G–poly C preference, which is not mirrored to the dA–poly dT over ct-DNA preference. In addition, **6** binds significantly stronger to ct-DNA, poly dA–poly dT and poly A–poly U in comparison to other studied compounds.

2.2 Thermal denaturation experiments

It is well known that upon heating ds-helices of polynucleotides at a well-defined temperature (T_m value) they dissociate into two single stranded polynucleotides. Non-covalent binding of small molecules to ds-polynucleotides usually has certain effect on the thermal stability of helices thus giving different T_m values. The difference between the ΔT_m value of free polynucleotide and the complex with a small molecule (ΔT_m value) is an important factor in characterisation of small molecule/ds-polynucleotide interactions.

The addition of any of the studied compounds strongly stabilised double helices of both DNA and RNA (Fig. 2, Table 3). A more detailed study of thermal stabilisation effects revealed strongly nonlinear dependence of ΔT_m values on the ratio r, suggesting saturation of binding sites at $r = 0.2$–0.3, which again is in good accord with calculated values of Scatchard ratio n (Table 2). All compounds stabilised poly

Table 2 Binding constants (log K_s)[a,b] and ratios n ([bound compound]/[polynucleotide phosphate]) calculated from the UV/Vis titrations of **4**, **5**, **6** and **7** with ds-polynucleotides at pH = 7.0 (buffer sodium cacodylate, $I = 0.05$ mol dm^{-3})

	poly dA–poly dT		poly A–poly U		poly G–poly C	
	log K_s	n	log K_s	n	log K_s	n
4	6.41	0.15	6.36	0.17	5.32	0.10
5	6.58	0.14	6.88	0.27	4.85	0.41
6	7.21	0.24	7.85	0.27	5.48	0.25
7	6.52	0.22	6.59	0.32	5.24	0.30

[a] Accuracy of $n \pm 10$–30%, consequently log K_s values vary in the same order of magnitude. [b] Titration data were processed according to the Scatchard equation.[9]

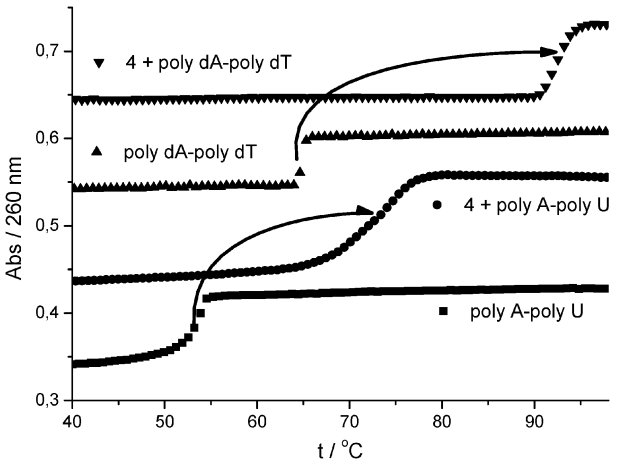

Fig. 2 Thermal denaturation of poly dA–poly dT and poly A–poly U upon addition of **4**. Ratio $r_{[compound]/[polynucleotide]}$ = 0.3, pH = 7.0 (buffer sodium cacodylate, I = 0.05 mol dm^{-3}).

dA–poly dT significantly more than its RNA analogue poly A–poly U. Intriguingly, thermal stabilisation of ct-DNA by **4–7** is 2–10 times weaker than stabilisation of poly dA–poly dT, and for compounds **4**, **5** and **7** it is even weaker than stabilisation of poly A–poly U. Such poly dA–poly dT over ct-DNA preference agrees roughly with correlations between corresponding binding constants (Table 2), and again points toward weaker binding of all studied compounds to G–C sequences.

2.3 Ethidium bromide displacement experiments

As an alternative method for comparison of the ability of the studied molecules to compete for binding with classical intercalators already bound to DNA/RNA,[11] we have performed ethidium bromide (**EB**) displacement assays (Fig. 3). Compounds **4–7** do not interact with **EB** under the experimental conditions used. According to DC_{50} values (Fig. 3A), **4–7** reveal comparable affinity toward poly dA–poly dT, while the DC_{50} values in Fig. 3B suggest that **6** and **7** bind somewhat stronger to poly A–poly U than **4** and **5**.

2.4 Circular dichroism (CD) experiments

So far, non-covalent interactions at 25 °C were studied by monitoring the spectroscopic properties of a studied compound upon the addition of the polynucleotides. In order to get insight into the changes of polynucleotide properties induced by small molecule binding, we have chosen CD spectroscopy as a highly sensitive method toward

Table 3 The ΔT_m[a] values (°C) of studied ds-polynucleotides upon addition of **4–7** at pH = 7.0 (buffer sodium cacodylate, I = 0.05 mol dm^{-3}), $r_{[compound]/[polynucleotide]}$ = 0.3

	ct–DNA[c]	poly dA–poly dT	poly A–poly U
4	6.6	27.6	20.5
5	3.1	> 36[b]	11.5
6	12.8	28.1	12.2
7	10.2	23.5	12.2

[a] Error in ΔT_m: ±0.5 °C.[10] [b] ΔT_m not possible to calculate since T_m is over 100 °C. [c] Published results.[6]

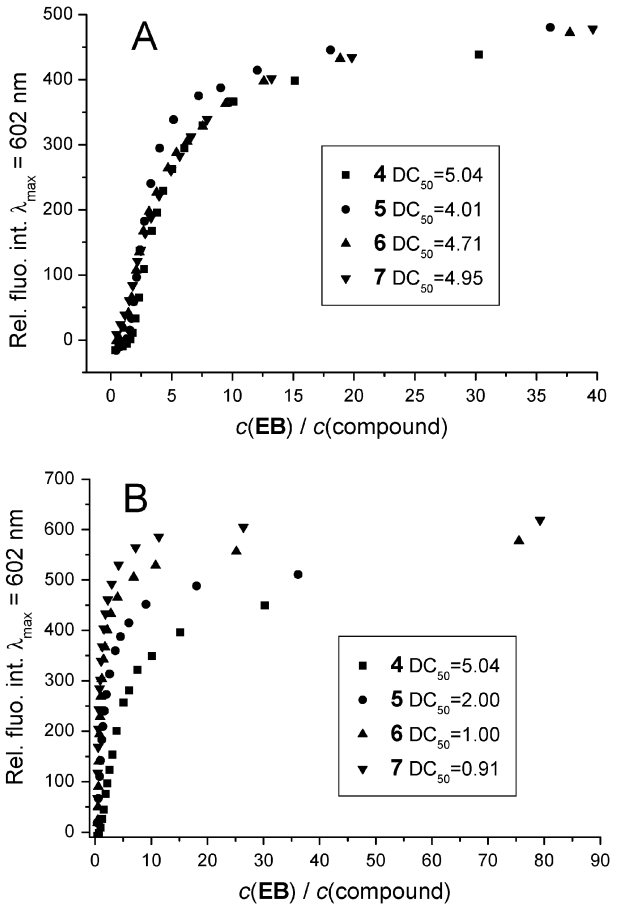

Fig. 3 Ethidium bromide (**EB**) displacement assay: poly dA–poly dT (A); poly A–poly U (B). To polynucleotide solution (c = 5 × 10^{-5} mol dm^{-3}), ethidium bromide (c = 1.5 × 10^{-5} mol dm^{-3}) was added (r ([**EB**]/[polynucleotide] = 0.3), and quenching of the **EB**/polynucleotide complex fluorescence emission (λ_{ex} = 520 nm, λ_{em} = 602 nm) was monitored as function of c(**EB**)/c(compound). The given DC_{50} values present the ratio c(**EB**)/c(compound) = [Int(**EB**/polynucleotide) − Int(**EB**$_{free}$)]/2, where Int(**EB**/polynucleotide) is fluorescence intensity of **EB**/polynucleotide complex and Int(**EB**$_{free}$) is fluorescence intensity of the free ethidium bromide before polynucleotide is added.

conformational changes in the secondary structure of polynucleotides.[12] In addition, achiral small molecules can eventually acquire induced CD spectra (ICD) upon binding to polynucleotides, which could give useful information about modes of interaction.[12] It should be noted that compounds **4–7** do not possess intrinsic CD spectra.

The addition of **4–7** resulted in a decrease of CD spectra of DNA/RNA polynucleotides (Fig. 4). Additionally, a strongly induced CD (ICD) band in the range λ = 300–500 nm appeared. Since UV/vis spectra of all studied compounds in the corresponding range are attributed to the absorption of the DBTAA moiety and the compounds do not exhibit intrinsic CD spectra, the observed ICD bands can also be attributed to the DBTAA moiety. Additionally, isoelliptic points in the ICD band range (λ = 300–500 nm) observed for all combinations of compounds and studied DNA/RNA strongly suggest one dominant interaction mode.[13] It is interesting to note that ICD spectra of **4–7** upon mixing with DNA (Fig. 4) are of similar

shape as those induced by addition of RNA, differing only in intensity and resolution of maxima and minima (Fig. 4). Such resemblance between DNA and RNA induced CD spectra of all compounds suggests analogous orientation of the DBTAA moiety with respect to the DNA/RNA chiral axis and thus most likely the same mode of binding.[12,14]

Strongly pronounced non-linear dependence of changes in CD spectra on the ratio r is pointing toward saturation of dominant binding sites at about r = 0.2–0.3. These r values are again in a good agreement with the ratios n obtained in UV/vis titrations (Table 2) as well as with the non-linear dependence of ΔT_m values on the ratio r in thermal melting experiments.

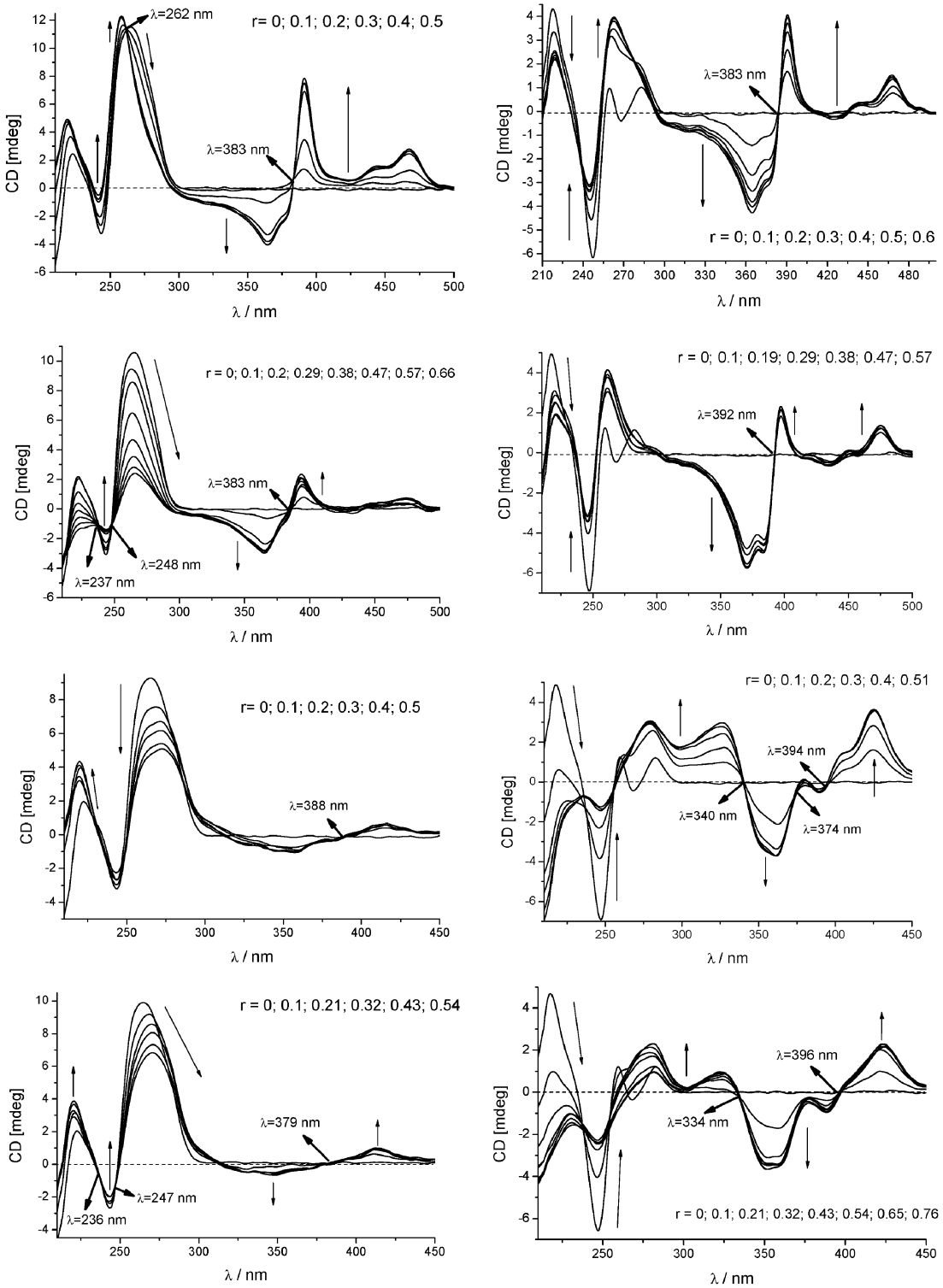

Fig. 4 CD titration of polynucleotides (c = 3.0 × 10^{-5} mol dm^{-3}) with **4**, **5**, **6** and **7** at molar ratios r = [compound]/[polynucleotide] (pH = 7.0, buffer sodium cacodylate, I = 0.05 mol dm^{-3}).

Intriguingly, ICD spectra of all compounds and polynucleotides are partially negative (300–380 nm) and partially positive (380–500 nm). According to the previously reported experiments and theoretical studies, an intercalated chromophore centered near the helix axis of double stranded polynucleotide should exhibit negative induced CD for all long-wavelength transitions polarized parallel to the long axis of the base-pair pocket, while transitions perpendicular to this direction, but still in the plane of the nucleobases (*i.e.*, parallel to the pseudo-dyad axis), should give positive CD.[15,16] Similar negative/positive ICD spectra were observed upon intercalation of 2,7-diazapyrene and its cations into various ds-DNA.[17] We can speculate that bulky side-chains of **5** and **7** are not likely to allow threading intercalation[18] with one of the side-chains positioned in the minor groove and the other in the major groove of double helix. In addition, fast equilibrium upon each mixing of DNA/RNA with compounds (less than 2 min) does not match threading intercalator association rates, which are characteristically much slower.[18] The other possible orientation, with both side-chains positioned in the same polynucleotide groove, would dictate orientation of the in-plane symmetry axis of DBTAA moiety connecting these two side-chains parallel to the long axis of the base-pair pocket and therefore would give a negative ICD band (300–380 nm), while transition within the DBTAA moiety perpendicular to this direction, but still in the plane of the nucleobases, should give a positive ICD band (380–500 nm). However, to provide accurate evidence for the proposed orientation of the DBTAA moiety within the intercalation binding site, additional LD and theoretical studies are needed,[15,16] whose complexity exceeds the scope of this work.

2.5 Viscometry measurements

The increase in DNA contour length that accompanies an intercalative mode of binding is most conveniently monitored by measuring the viscosity of sonicated rodlike fragments of DNA as a function of ligand binding ratio, *r*. Cohen and Eisenberg have deduced that the relative increase in contour length in the presence of bound drug is approximated by the cube root of the ratio of the intrinsic viscosity of the DNA-drug complex to that of the free DNA (equation in the ESI†).[19] Classical monointercalators like ethidium bromide, proflavine and 9-aminoacridine have values of helix extension parameter (viscosity index), α, of about 0.8–0.9 while extension parameters of bisintercalators are usually in the range 1.5–1.9. On the other hand, molecules like groove binders which do not insert between base pairs, in general do not elongate the DNA double helix and therefore yield no or very small viscosity increases.

Viscometry experiments (ESI†) performed with ct-DNA yielded values of $\alpha = 0.93 \pm 0.03$ (**4**), 1.08 ± 0.04 (**6**) and 0.96 ± 0.1 (**7**), which agree well with the value obtained for ethidium bromide (α(**EB**) $= 0.84 \pm 0.05$). Experiment with **5** was hampered by precipitation upon first addition of compound to ct-DNA. Obtained values strongly support intercalation of studied compounds into ds-DNA as the dominant binding mode.[20]

2.6 Discussion of DNA/RNA binding studies

According to the results of all the applied methods, **4**, **5**, **6** and **7** strongly bind to both ds-DNA and ds-RNA, most likely by the same mode of interaction. Strong hypochromic and bathochromic effects in UV/vis titrations (Table 1), high affinity (Table 2), strong thermal stabilisation of both DNA and RNA (Table 3) and similar ICD spectra upon DNA and RNA addition, all strongly support intercalation as a dominant binding mode for all the studied compounds and polynucleotides.[20]

Binding constants (Table 2) and thermal denaturation studies (Table 3) point toward significantly stronger interactions of **4–7** with A–T(U) sequences in comparison to G–C sequences. Most classical intercalators do not differ between A–T(U) sequences and G–C sequences or in some cases show weak preference toward G–C sequences. One of the major differences between A–T(U) and G–C sequences is the amino group of guanine protruding into the minor groove of the double helix and sterically hindering non-covalent interactions of small molecules, *e.g.* minor groove binders. Most likely interactions of the positively charged side-chains of the studied compounds within the minor groove are analogously affected, thus resulting in the observed A–T(U) over G–C preference. Furthermore, stronger thermal stabilization of poly dA–poly dT in comparison to RNA analogue (poly A–poly U) can be attributed to the much narrower and hydrophobic minor groove of the ds-DNA with respect to ds-RNA.[21] That observation points to the fact that side chains of **4**, **5**, **6** and **7** form additional binding interactions only within the minor groove of ds-DNA, and moreover these interactions are suppressed by the presence of G–C basepairs (therefore G–C basepair containing ct-DNA was stabilized less than RNA poly A–poly U).

2.7 Evaluation of the antiproliferative effect of 4, 5, 6 and 7 *in vitro*

Many of the currently used antitumor drugs base their activity on intercalation or minor groove binding to cellular DNA. Since **4–7** intercalate into DNA and form additional binding interactions by side-chains within the minor groove of ds-DNA, we investigated their effects on the proliferation of different human tumor cell lines. The obtained results (Table 4) clearly point to the correlation between antiproliferative activity and the structure of a side-chain attached to DBTAA moiety. Namely, **4** and **7**, characterized by aliphatic, flexible side-chains, are by far less active against HCT 116, SW 620, H 460 cell lines than **5** and **6**, possessing aromatic, sterically demanding side-chains. The exception is the selectivity of **4** and **7** toward PC-3, MCF-7 and a non-tumor cell line HaCaT, which is quite intriguing. On the other hand, **5** and **6** exhibited similar activity toward all cell lines. Different characteristics of aromatic positive charge *vs.* aliphatic positive charge (*e.g.* hydrophobicity-related cellular uptake, or different intercellular targets/pathways) can be responsible for the observed biological effects. Namely, the act of intercalation *per se* induces local structural changes (*e.g.* unwinding of the double helix and lengthening of the DNA strand) to the DNA, which leads to the inhibition of transcription and

Table 4 *In vitro* inhibition of compounds **4–7** on the growth of tumor cells

	$IC_{50}/\mu M^a$					
Compd	PC-3	HCT 116	SW 620	MCF-7	H 460	HaCaT
4	19 ± 16	≥ 100	≥ 100	6 ± 5	≥ 100	≥ 100
5	13 ± 2	29 ± 4	3 ± 1	4 ± 3	5 ± 3	1 ± 0.5
6	5 ± 0.8	10 ± 2	15 ± 7	4 ± 2	9 ± 1	15 ± 8
7	35 ± 6	71 ± 5	39 ± 14	12 ± 9	32 ± 5	90 ± 0.1

[a] IC_{50}: the concentration that causes a 50% reduction of the cell growth.

replication.[22] However, the presence of a cationic substituent on the molecule may increase DNA residence time which, in turn, may increase the (geno)toxicity of that compound. If the intercalation brings an electrophilic center in proximity to the DNA, a covalent bond (DNA adduct) may form. Such intercalating compounds are usually the most genotoxic. Still, in mammalian cells the stabilization of DNA double strand breaks arising as a consequence of DNA topoisomerase II (topo II) poisoning, usually accounts for the clinical antitumor activity of intercalating drugs such as doxorubicin (DOX) and m-amsacrine. Minor changes to the compound structures can result in reduction or complete loss of antitumor activity and/or genotoxicity thus indicating the complexities of chemical/DNA/topo II ternary interactions.[23]

Many clinically useful drugs exert their cytotoxic effects through poisoning of either topo I or topo II. Topoisomerase-active drugs either inhibit the ability of the enzymes to initially cleave DNA (catalytic inhibitors) or stabilise the fragile and normally transient 'cleavable complexes' they form by preventing strand religation (poisons). No overall structure–activity relationships are discernible for this property, but small structural changes within a particular series appear to markedly alter the relative activities of analogues towards the two enzymes. This observation supports the 'drug stacking' model of interaction, where inhibitors with a 'deep intercalation mode' are responsible for topo I-mediated cleavage and those with an 'outside binding mode' are responsible for topo II-mediated cleavage.[24] Although additional experiments (*e.g.* inhibition of topoisomerases, cell cycle perturbation studies, *etc.*) are necessary for the accurate elucidation of differences in biological activity of **4**, **5**, **6** and **7**, it is evident that different cationic side-chains markedly influence the activity (cytotoxicity) of these compounds, whereby **5** and **6** (characterised by sterically hindered positive charge on side chain) are obviously more nonselectively cytotoxic (probably inducing DNA strand breaks through topoisomerase poisoning), while **4** and **7** (exposed positive charges on side chains) are selective and thus represent interesting lead molecules.

3. Conclusions

Although the cationic DBTAA derivatives studied here structurally resemble the analogous dicationic porphyrins, several differences are observed, like the absence of any significant self-stacking of DBTAA derivatives in aqueous medium.[6,8] Moreover, DBTAA derivatives form only one dominant type of complex with DNA/RNA at conditions of an excess of polynucleotide, whereby each DBTAA molecule is bound independently to the DNA/RNA binding site, at variance to porphyrins which often agglomerate along polynucleotides and form more different complexes.[25,26] Compounds **4–7** most likely intercalate into ds-DNA and ds-RNA, and their positively charged side-chains additionally interact within the minor groove of polynucleotides, contributing to the overall affinity of the compounds and controlling pronounced A–T(U) over G–C sequence preference, as well as stronger thermal stabilization of ds-DNA than ds-RNA. Furthermore, all compounds showed moderate to high antiproliferative activity against the human tumour cell lines, whereby clear correlation between the structure of the side-chain and cytotoxic activity was observed. Such an impact of positively charged DBTAA side-chains on the interactions with DNA/RNA as well as on the antiproliferative activity offers an intriguing and simple synthetic approach to the modulation and fine tuning of DNA/RNA binding properties and biological activity of DBTAA-derivatives. For instance, an introduction of a number of DNA/RNA active substituents to the DBTAA side-chains is in progress.

4. Materials and methods

4.1 Spectroscopic experiments

The electronic absorption spectra were obtained on a Varian Cary 100 Bio spectrometer, CD spectra on a JASCO J815 spectrophotometer and fluorescence spectra on the Varian Eclipse fluorimeter, all in quartz cuvettes (1 cm). The spectroscopic studies were performed in aqueous buffer solution (pH = 7, sodium cacodylate buffer, I = 0.05 mol dm^{-3}). Under the experimental conditions, absorbance of **4**, **5**, **6**, **7** was proportional to their concentrations. Polynucleotides were purchased as noted: poly A–poly U, poly G–poly C, poly dA–poly dT, (Sigma), calf thymus (*ct*)-DNA (Aldrich). Polynucleotides were dissolved in sodium cacodylate buffer, I = 0.05 mol dm^{-3}, pH = 7. Calf thymus (*ct*-) DNA was additionally sonicated and filtered through a 0.45 μm filter.[27,28] Polynucleotide concentration was determined spectroscopically[28] as the concentration of phosphates. Spectroscopic titrations were performed by adding portions of polynucleotide solution into the solution of the studied compound.

Obtained data were corrected for dilution. Titration data were processed by the Scatchard equation.[9] Values for K_s and n given in Table 2 all have satisfactory correlation coefficients (> 0.999). Thermal melting curves for DNA, RNA and their complexes with studied compounds were determined, as previously described,[28,29] by following the absorption change at 260 nm as a function of temperature. Absorbance of the ligands was subtracted from every curve, and the absorbance scale was normalized. The T_m values are the midpoints of the transition curves, determined from the maximum of the first derivative and checked graphically by the tangent method.[28] ΔT_m values were calculated by subtracting the T_m of the free

nucleic acid from the T_m of the complex. Every ΔT_m value here reported was the average of at least two measurements, the error in ΔT_m is $\pm$ 0.5 °C.

Ethidium bromide (**EB**) displacement assay: to polynucleotide solution ($c = 5 \times 10^{-5}$ mol dm^{-3}) ethidium bromide ($c = 1.5 \times 10^{-5}$ mol dm^{-3}) was added (r ([**EB**]/[polynucleotide] = 0.3), and quenching of the **EB**/polynucleotide complex fluorescence emission (λ_{ex} = 520 nm, λ_{em} = 601 nm) was monitored as function of c(**EB**)/c(compound). The given IC_{50} values represent the ratio c(**EB**)/c(compound) = [Int(**EB**/polynucleotide) − Int(**EB**$_{free}$)]/2, where Int(**EB**/polynucleotide) is the fluorescence intensity of **EB**/polynucleotide complex and Int(**EB**$_{free}$) is the fluorescence intensity of the free ethidium bromide before polynucleotide is added.

Viscometry measurements were conducted with an Ubbelohde viscometer system AVS 350 (Schott). The temperature was maintained at 25 ± 0.1 °C. Aliquots of drug stock solutions were added to 5.5 ml of × 10^{-4} mol dm^{-3} *ct*-DNA solution in sodium cacodylate buffer, I = 0.05 mol dm^{-3}, pH = 7, with a compound to DNA phosphate ratio r less than 0.2. Dilution never exceeded 4% and was corrected for in the calculations. The flow times were measured at least five times optically with a deviation of ±0.2 s. The viscosity index α was obtained from the flow times at varying r according to the following equation:[30]

$$L/L_0 = [(t_r - t_0)/(t_{DNA} - t_0)]^{1/3} = 1 + \alpha r$$

whereby t_0, t_{DNA} and t_r denote the flow times of buffer, free DNA and DNA complex at reagent/phosphate ratio r, respectively; L/L_0 is the relative DNA lengthening. The L/L_0 to r-plot was fitted to a straight line that gave slope α. The error in α is ≤0.1.

4.2 Biological assays

Antiproliferative assays. The experiments were carried out on 5 human cell lines, which are derived from 5 cancer types. The following cell lines were used: PC-3 (prostatic carcinoma), MCF-7 (breast carcinoma), SW 620 and HCT 116 (colon carcinoma), H 460 (lung carcinoma) and HaCaT (immortalized human skin keratinocytes). The cells were cultured as monolayers and maintained in Dulbecco's modified Eagle's medium (DMEM) supplemented with 10% fetal bovine serum (FBS), 2 mM L-glutamine, 100 U ml^{-1} penicillin and 100 μg ml^{-1} streptomycin in a humidified atmosphere with 5% CO_2 at 37 °C. The growth inhibition activity was assessed according to the slightly modified procedure performed at the National Cancer Institute, Developmental Therapeutics Program.[31,32] The cells were inoculated onto standard 96-well microtiter plates on day 0. The cell concentrations were adjusted according to the cell population doubling time (PDT). Test agents were then added in five consecutive 10-fold dilutions (10^{-8} to 10^{-4} mol l^{-1}) and incubated for further 72 h. Working dilutions were freshly prepared on the day of testing. After 72 h of incubation, the cell growth rate was evaluated by performing the MTT assay, as previously described.[31] Each test point was performed in quadruplicate in three individual experiments. The results are expressed as IC_{50}, which is the concentration necessary for 50% of inhibition. The IC_{50} values for each compound are calculated from dose-response curves using linear regression analysis.

Acknowledgements

Support for this study by the Ministry of Science, Education and Sport of Croatia (Projects 98-0982914-2918, 098-0982464-2514) and by the Grant (WCh-BW) from the Jagiellonian University, Krakow, Poland, is gratefully acknowledged.

References

1 R. B. Silverman, in *The Organic Chemistry of Drug Design and Drug Action*, Elsevier Academic, Burlington, MA, 2004.
2 M. Demeunynck, C. Bailly and W. D. Wilson, in *DNA and RNA Binders*, ed. Wiley-VCH, Weinheim, 2002.
3 M. Maiti and G. S. Kumar, *Med. Res. Rev.*, 2007, **27**, 649–695.
4 For reviews see *e.g.*: B. Meunier, A. Robert, G. Pratviel and J. Bernadou, in *The Porphyrin Handbook*, ed. K. M. Kadish, K. Smith and R. Guilard, Academic Press, San Diego, CA, 1999, vol. 4, pp. 119–187; R. K. Pandey and G. Zheng, in *The Porphyrin Handbook*, ed. K. M. Kadish, K. Smith and R. Guilard, Academic Press, San Diego, CA, 1999, vol. 6, pp. 157–230.
5 L. G. Marzilli, *New J. Chem.*, 1990, **14**, 409–420; R. J. Fiel, *J. Biomol. Struct. Dyn.*, 1989, **6**, 1259–1275; R. F. Pasternack and E. J. Gibbs, *Met. Ions Biol. Syst.*, 1996, **33**, 367–397.
6 D. Pawlica, M. Radić Stojković, L. Sieroń, I. Piantanida and J. Eilmes, *Tetrahedron*, 2006, **62**, 9156–9165.
7 M. Radić Stojković, I. Piantanida, M. Kralj, M. Marjanović, M. Žinić, D. Pawlica and J. Eilmes, *Bioorg. Med. Chem.*, 2007, **15**, 1795–1801.
8 D. Pawlica, M. Radić Stojković, Ł. Dudek, I. Piantanida, L. Sieroń and J. Eilmes, *Tetrahedron*, 2009, **65**, 3980–3989.
9 G. Scatchard, *Ann. N. Y. Acad. Sci.*, 1949, **51**, 660–672; J. D. McGhee and P. H. von Hippel, *J. Mol. Biol.*, 1976, **103**, 679–684.
10 I. Piantanida, B. S. Palm, M. Žinić and H.-J. Schneider, *J. Chem. Soc., Perkin Trans. 2*, 2001, 1808–1816.
11 D. L. Boger, B. E. Fink, S. R. Brunette, W. C. Tse and M. P. Hedrick, *J. Am. Chem. Soc.*, 2001, **123**, 5878–5891.
12 A. Rodger and B. Norden, in *Circular Dichroism and Linear Dichroism*, Oxford University Press, New York, 1997, ch. 2.
13 N. Berova, K. Nakanishi and R. W. Woody, in *Circular dichroism Principles and Applications*, Wiley-VCH, New York, 2nd edn, 2000.
14 M. Eriksson and B. Nordén, *Methods Enzymol.*, 2001, **340**, 68–98.
15 R. Lyng, A. Rodger and B. Nordén, *Biopolymers*, 1991, **31**, 1709–1820.
16 P. E. Schipper, B. Norden and F. Tjerneld, *Chem. Phys. Lett.*, 1980, **70**, 17–21; B. Norden and F. Tjerneld, *Biopolymers*, 1982, **21**, 1713–1734.
17 H. C. Becker and B. Norden, *J. Am. Chem. Soc.*, 1997, **119**, 5798–5803.
18 R. S. Lokey, Y. Kwok, V. Guelev, C. J. Pursell, L. H. Hurley and B. L. Iverson, *J. Am. Chem. Soc.*, 1997, **119**, 7202–7210.
19 L. P. G. Wakelin, *Med. Res. Rev.*, 1986, **6**, 275.
20 E. C. Long and J. K. Barton, *Acc. Chem. Res.*, 1990, **23**, 271–279; G. Dougherty and J. R. Pilbrow, *Int. J. Biochem.*, 1984, **16**, 1179–1192.
21 C. R. Cantor and P. R. Schimmel, in *Biophysical Chemistry*, WH Freeman, San Francisco, CA, 1980, pp. 1109–1181.
22 L. R. Ferguson and W. A. Denny, *Mutat. Res., Fundam. Mol. Mech. Mutagen.*, 2007, **623**, 14–23.
23 R. D. Snyder and M. R. Arnone, *Mutat. Res., Fundam. Mol. Mech. Mutagen.*, 2002, **503**, 21–35.
24 W. A. Denny, *Expert Opin. Invest. Drugs*, 1997, **6**, 1845–1852.
25 K. Prochazkova, Z. Zelinger, K. Lang and P. Kubat, *J. Phys. Org. Chem.*, 2004, **17**, 890–897.

26 A. A. Ghazaryan, Y. B. Dalyan, S. G. Haroutiunian, A. Tikhomirova, N. Taulier, J. W. Wells and T. V. Chalikian, *J. Am. Chem. Soc.*, 2006, **128**, 1914–1921.
27 J. B. Chaires, N. Dattagupta and D. M. Crothers, *Biochemistry*, 1982, **21**, 3933–3940.
28 B. S. Palm, I. Piantanida, M. Žinić and H. J. Schneider, *J. Chem. Soc., Perkin Trans. 2*, 2000, 385–392.
29 J.-L. Mergny and L. Lacroix, *Oligonucleotides*, 2003, **13**, 515–537.
30 G. Cohen and H. Eisenberg, *Biopolymers*, 1969, **8**, 45; M. Wirth, O. Buchardt, T. Koch, P. E. Nielsen and B. Nordén, *J. Am. Chem. Soc.*, 1988, **110**, 932.
31 K. Ester, M. Hranjec, I. Piantanida, I. Ćaleta, I. Jarak, K. Pavelić, M. Kralj and G. Karminski-Zamola, *J. Med. Chem.*, 2009, **52**, 2482–2492.
32 M. R. Boyd and K. D. Paull, *Drug Dev. Res.*, 1995, **34**, 91–109.